Revisiting the temperature dependence of protein diffusion inside bacteria: validity of the Stokes-Einstein equation

Asmaa A. Sadoon[a,b,d], William F. Oliver[a,b], and Yong Wang[a,b,c,*]

[a] Department of Physics, [b] Materials Science & Engineering Program, [c] Cell and Molecular Biology Program, University of Arkansas, Fayetteville, Arkansas, 72701, USA. [d] Department of Physics, University of Thi-Qar, Thi-Qar, Iraq.

*Corresponding author: yongwang@uark.edu

Abstract

Although the transport and mixing of proteins and other molecules inside bacteria rely on the diffusion of molecules, many aspects of the molecular diffusion in bacterial cytoplasm remain unclear or controversial, including how the diffusion-temperature relation follows the Stokes-Einstein equation. In this study, we applied single-particle tracking photoactivated localization microscopy (sptPALM) to investigate the diffusion of histone-like nucleoid structuring (H-NS) proteins and free dyes in bacterial cytoplasm at different temperatures. Although the diffusion of H-NS proteins in both live and dead bacteria increased at higher temperatures and appeared to follow the Arrhenius equation, the diffusion of free dyes decreased at higher temperatures, questioning the previously proposed theories based on superthermal fluctuations. To understand the measured diffusion-temperature relations, we developed an alternative model, in which the bacterial cytoplasm is considered as a polymeric network / mesh. In our model, the Stokes-Einstein equation remains valid, while the polymeric network contributes a significant term to the viscosity experienced by the molecules diffusing in bacterial cytoplasm. Our model was successful in predicting the diffusion-temperature relations for both H-NS proteins and free dyes in bacteria. In addition, we systematically examined the predicted diffusion-temperature relations with different parameters in the model, and predicted the possible existence of phase transitions.

Keywords: diffusion-temperature relation, super-resolution fluorescence microscopy, single-particle tracking, Brownian motion

Text

It is important to understand molecular diffusion inside bacteria due to its critical role in transporting and mixing various molecules in bacteria [1]. The molecular diffusion inside bacteria is also physically interesting because (1) bacterial cytoplasm is highly complex, crowded, and full of biological macromolecules, polymers, and filaments [2,3], and (2) various active cellular processes occur constantly inside bacteria, driving the bacterial cytoplasm far from thermodynamic equilibrium [1]. However, the small size of bacteria and high copy-number of proteins make it challenging to study the diffusive dynamics of individual proteins in bacteria [4,5] until the recent development of techniques that combine super-resolution fluorescence microscopy and single-particle tracking or correlation spectroscopy [6–13].

The temperature (T) dependence of molecular diffusion coefficient (D) is commonly described by the renowned Stokes-Einstein equation ($D \propto k_BT/6\pi\eta r$) for molecules with Brownian motion [14,15] and the fluctuation-dissipation theorem [16]. However, the Stokes-Einstein equation has been challenged for molecules in live systems where active processes happen constantly [17]. Recent work in both eukaryotic cells and bacteria showed that active biological processes led to enhanced molecular diffusions [18,19]. Weber et al. measured the diffusion of DNA loci in live *E. coli* and yeast at different temperatures and observed that the diffusion-temperature relation followed the Arrhenius equation, $D \propto exp(-E_a/k_BT)$, instead of the Stokes-Einstein equation [17]. It was proposed that the observed Arrhenius D–T relation was due to the ATP-dependent super-thermal fluctuations [17]. However, the validity of the ATP-dependent super-thermal theory remains questionable for several reasons. First, the role of temperature-dependent viscosity has not been ruled out experimentally [17]. Second, a similar Arrhenius D–T relation has been observed for lipid molecules in both cellular membranes and artificial lipid bilayers without ATP [20–23]. Therefore, the origin of the observed non-Stokes-Einstein D–T relation and validity of the Stokes-Einstein equation for molecules in live systems remain controversial.

In this work, we revisited the temperature dependence of molecular diffusion in bacteria and the validity of the Stokes-Einstein equation. We applied single-particle tracking photoactivated localization microscopy (sptPALM) [6] to measure the dynamic diffusion of histone-like nucleoid structuring (H-NS) proteins in both live and dead *E. coli* at different temperatures. H-NS is one of the DNA binding proteins in *E. coli*, regulating ~5% of the bacterial genome [24]. SptPALM imaging was performed as described previously [7,8] and in the Supplementary Information, while the temperature was modulated from 21 ºC to 37 ºC by a stage-top incubator. Trajectories of H-NS proteins were similar to those observed previously: some trajectories were localized while other proteins traveled large distances [7,8] (SI Fig. 1&2). Dead bacteria were obtained by electric shock (electroporation with 1.9 kV and 5 ms) [25]; staining of the treated bacteria by SYTOX™ Blue dyes confirmed that ~90% of the cells were dead (SI Fig. 3). From the identified trajectories of the proteins (SI Fig. 1), we calculated the mean-square-displacement (MSD), $MSD\ (\tau) = \langle (r(t+\tau) - r(t))^2 \rangle$, where $r(t)$ is the position of the molecules and the τ is the lag time. Consistent with previous results [7,8], the MSD curves at different temperatures were nonlinearly bending down, indicating the sub-diffusion of the H-NS proteins (Fig. 1A&B). Compared to the room temperature (21 ºC) data, the MSD curves were continuously higher as temperature increased, suggesting faster diffusion at higher

temperatures. We also observed that the MSD curves were lower in dead bacteria, indicating that the proteins were slower in the dead bacteria. We then fitted the MSD curves individually to $MSD = 4D\tau^{\alpha}$, where D is the generalized diffusion coefficient and α is the sub-diffusive scaling exponent, and confirmed that D increased as the temperature increased (green circles, Fig. 1C), whereas α did not significantly depend on the temperature (~0.3–0.5, SI Fig. 4). The diffusion-temperature relation of H-NS proteins in both live and dead *E. coli* did not follow the Stokes-Einstein equation (i.e., $D \propto T$ for constant η; red dotted lines, Fig. 1C). Instead, the data could be fitted by the Arrhenius equation, $D = D_0\, exp(-E_a/k_BT)$ (black dashed lines in Fig. 1C; also see SI Fig. 5), where E_a is the "activation" energy and k_B is the Boltzmann constant. Similar observations for the diffusion of DNA loci in *E. coli* and yeast were attributed to the ATP-dependent super-thermal fluctuations [17]. However, we found it unexpected that the "activation" energy of the H-NS proteins in dead bacteria (25±4 kJ/mol) was 79% higher than that in live ones (14±6 kJ/mol).

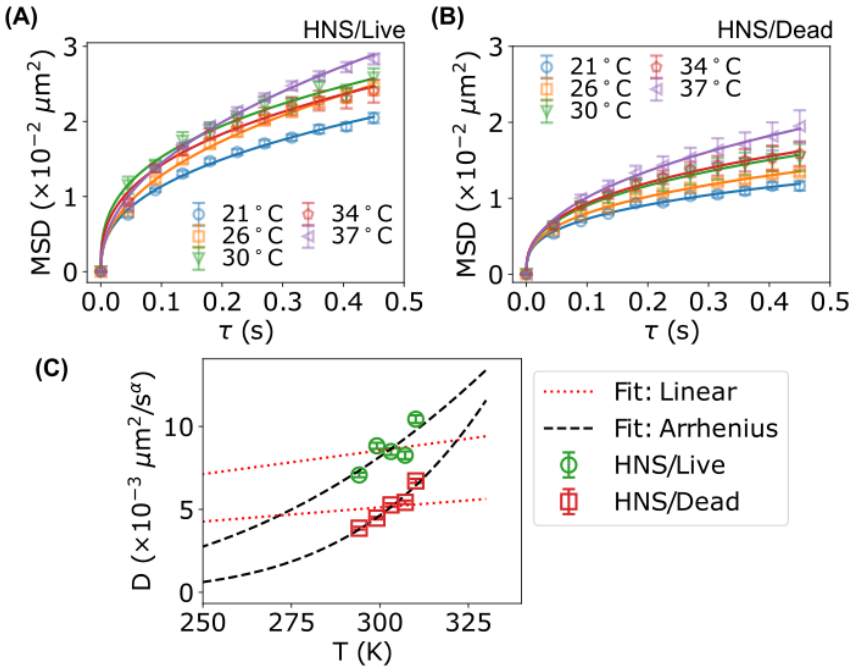

Figure 1: Temperature dependence of H-NS diffusion in live and dead *E. coli*. (**A, B**) MSD of H-NS in (**A**) live and (**B**) dead *E. coli* at different temperatures. Dashed lines are fitted curves using $MSD = 4D\tau^{\alpha}$. Error bars represent standard errors of the means (SEM). (**C**) Dependence of the generalized diffusion coefficient of H-NS proteins in live (green circles) and dead (red squares) *E. coli*. Error bars stand for fitting errors. Red dotted lines are fittings with linear equations, while black dashed lines are fittings with the Arrhenius equation.

We further pursued the validity of the ATP-dependent superthermal theory by hypothesizing that, if the theory were true, the diffusion of free dyes in bacteria would follow the same temperature dependence as

the H-NS proteins. We introduced photoactivatable dyes (PA Janelia Fluor 646) into *E. coli* by electroporation (1.9 kV, 5 ms) [25], which killed most of the bacteria but successfully delivered the dyes into the bacteria. We then performed the same sptPALM measurements and analysis for the free-dye diffusion. Similar to H-NS, the diffusion of the dyes was subdiffusive (Fig. 2A), confirming the crowding and confining properties of bacterial cytoplasm [7,11,12,26]. However, surprisingly, the MSD values of the free dyes were lower at higher temperatures than the room temperature (Fig. 2A). A negative relation was confirmed by plotting the fitted diffusion coefficients *vs.* temperature (Fig. 2B and SI Fig. 5). This negative relation could be fitted by the Arrhenius equation; however, the fitted "activation" energy was negative (-14+/-5 kJ/mol).

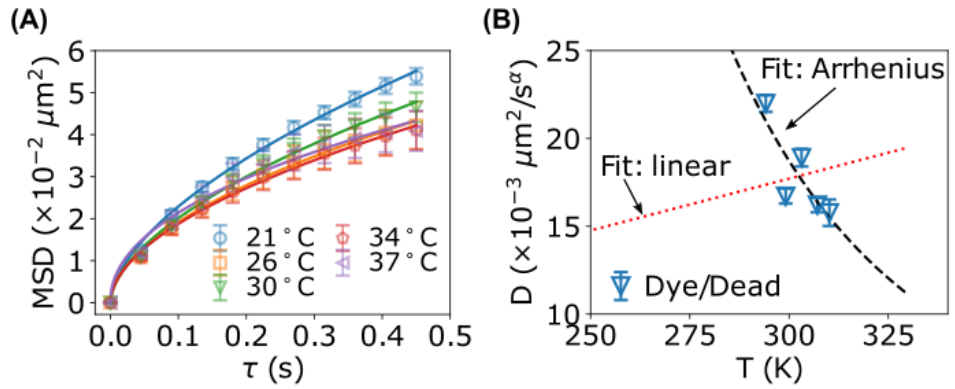

Figure 2: Temperature dependence of free-dye diffusion in dead *E. coli*. (**A**) MSD of dyes in dead *E. coli* at different temperatures. Dashed lines are fitted curves using $MSD = 4D\tau^{\alpha}$. Error bars represent SEM. (**B**) Dependence of the generalized diffusion coefficient of dyes in dead *E. coli*. Error bars stand for the fitting errors. Red dotted line is a linear fitting, while black dashed line is a fitting with the Arrhenius equation.

In an attempt to develop a model to understand the observed temperature dependence of the diffusion of both H-NS proteins and free dyes in *E. coli*, we were inspired by the temperature dependence of lipids' diffusion. It was reported that the diffusion-temperature relation of lipids followed the Arrhenius equation in both cellular membranes and artificial lipid bilayers without ATP [20–23], which was explained by the free-area or free-volume theory. In the free-volume theory, a lipid molecule could diffuse/hop to a next location if (1) it has sufficient energy to overcome the attractive forces from its neighbors and (2) an empty site is available [20]. This theory predicted the desired temperature dependencies of the viscosity and the diffusion coefficient of the lipids, while assuming the Stokes-Einstein equation remained valid [20–23].

Our model for understanding the diffusion-temperature relation of molecules inside bacterial cytoplasm is derived from the free-volume theory [20]. Briefly, we consider the bacterial cytoplasm as a network made of various polymers, including nucleic acids, polysaccharides, polyamides, polyester, and

polyanhydrides [27]. Therefore, the bacterial cytoplasm is split into small meshes [28,29], and the movements of molecules inside bacterial cytoplasm are hindered by the polymeric network. The hindrance may contribute to additional "viscosity" for bacterial cytoplasmic molecules: (1) if a molecule interacts with the network (e.g., H-NS proteins bind to DNA [24]), it requires sufficient energy to overcome these interactions before diffusion (note that this activation energy is a mean-field parameter for both bound and unbound H-NS proteins); (2) an empty mesh site is needed to be so that the molecule can move to. This argument resembles that of the free-volume theory for lipid diffusion [20–23], allowing us to apply the established equations directly to the additional viscosity experienced by molecules diffusing inside bacterial cytoplasm, with slight modifications of the interpretations of the variables:

$$\eta = A\,T e^{E_a/k_B T + \gamma v_m/(v - v_m)}$$

where A is temperature dependent but far less than the exponential term, E_a the "activation" energy, k_B the Boltzmann constant, T the temperature, v the mesh size (volume) of the network, v_m the close-packed molecular volume, and γ a correction factor [20]. We emphasize that this "additional viscosity" is a term due to the polymeric network/mesh, while there also exist contributions to the "full viscosity" from other molecules (e.g., water, and globular macromolecules [30]).

For a given molecule, we expect that the close-packed molecular volume v_m is constant and essentially temperature-independent in the small experimental range (21 ºC – 37 ºC). However, the mesh size of polymeric networks v is likely temperature-dependent are much larger than the molecular volume [28]. For example, the mesh size of a polymeric κ-carrageenan network was measured to decrease as temperature increases [29]. From this experimental result and due to the small temperature range in this study, we assume the simplest linear relation for the temperature dependence of the mesh size of bacterial cytoplasm, $v = v(T) = v_0 - \xi\, T = -\xi\,(T - T_0)$, where $\xi = -\frac{dv}{dt}$ is the unnormalized thermal contraction coefficient and T_0 the extrapolated temperature intercept. We expect that the assumption of linear v–T relation is only valid in a small temperature range and thus it is likely that T_0 is not physically meaningful. If we simplify the constants by redefining $T_m = \gamma v_m/\xi$ and $T_c = T_0 - v_m/\xi$, we have

$$\eta = A\,T e^{E_a/k_B T - T_m/(T - T_c)}$$

Plugging this temperature-dependent viscosity to the Stokes-Einstein equation, we get

$$D = \frac{k_B T}{6\pi\eta r} = D_0\, e^{-E_a/k_B T + T_m/(T - T_c)}$$

where $D_0 = k_B/6\pi A r$ is again temperature dependent but far less than the exponential term, and r the radius of the diffusing molecule.

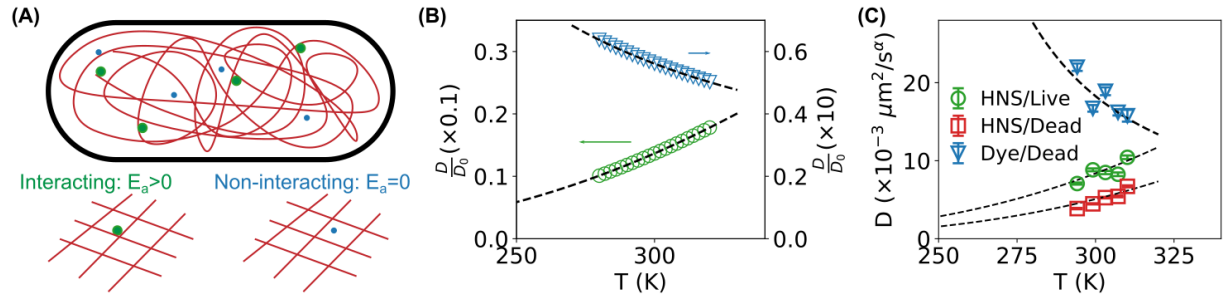

Figure 3. Model of additional "viscosity" experienced by molecules in a polymeric network. (**A**) Sketch of the model for two types of molecules: interacting (green, E_a>0) or non-interacting (blue, E_a=0) with the network. (**B**) Predicted temperature-dependence of the diffusion coefficients from the theory for interacting (green, E_a=15 kJ/mol) and non-interacting (blue, E_a=0 kJ/mol) molecules. Black dashed lines are fittings using the Arrhenius equation. (C) Overlapping of model-predicted *D-vs-T* curves (black dashed lines) and experimental data (colored symbols).

The main difference between H-NS proteins and free dyes in our model is that H-NS proteins can bind to the polymeric network (e.g., DNA) [24,31] while the dyes do not. As a result, H-NS proteins need to overcome an "activation" energy and unbind from the network before they diffuse. However, the free dyes do not have such a prerequisite. Therefore, we have $E_a > 0$ for the H-NS proteins but $E_a = 0$ for the dyes. To visualize the predictions from our models, we plotted, in Fig. 3B, the diffusion coefficients at different temperatures for two types of molecules: E_a = 15 kJ/mol for a molecule that interacts with the polymeric network, and E_a = 0 kJ/mol for a non-interacting molecule. The other parameters in the model were kept the same (T_m = 500 K, T_c = 10 K) for both molecules. The model predicted two different diffusion-temperature relations, which resembled the experimental results: the diffusion coefficient increased at higher temperatures for the interacting molecules (green circles in Fig. 3B), but decreased for the non-interacting molecules (blue squares in Fig. 3B). In addition, both curves could be fitted well by the Arrhenius equation (black dashed lines in Fig. 3B).

To assess the consistency of the model-predictions with the experimental results, we overlapped model-predicted curves on the experimental data in Fig. 3C. For the two curves for H-NS proteins (Fig. 3C), T_m = 500 K and T_c = 10 K were kept the same, as they shared the same molecular volume (v_m); however, the activation energies were chosen as $E_a = 3.0\times10^{-20}$ J or 18 kJ/mol for H-NS proteins in live bacteria and $E_a = 3.2\times10^{-20}$ J or 19 kJ/mol for in dead bacteria. For the curve of the dyes (Fig. 3C), we reduced T_m to 350 K and increased T_c to 160 K ($T_m \propto v_m$ and $T_c = T_0 - v_m/\xi$) due to the smaller size of the dyes, and applied E_a = 0 J. We highlight that the model-predicted curves matched well with the experimental data. On the other hand, we note that, due to the narrow temperature range of the experiments, it is practically difficult to fit the experimental data and reliably extract the parameters, as multiple sets of parameters could fit the data well (SI Fig. 6).

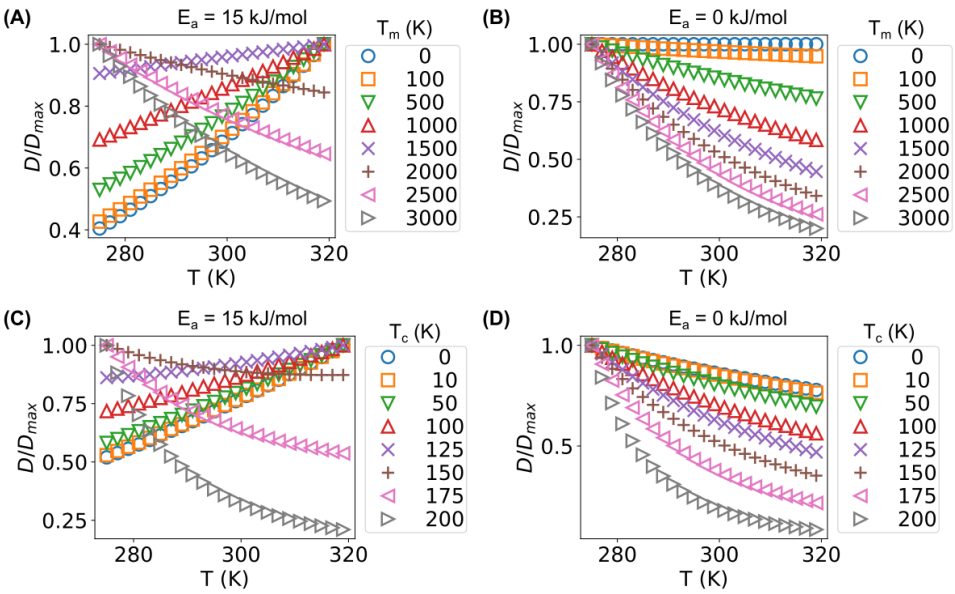

Figure 4. Temperature dependence of diffusion coefficients of molecules in polymeric networks with different parameters. (**A**) Varying T_m while keeping T_c = 10 K and E_a = 15 kJ/mol constant. (**B**) Varying T_m, while keeping T_c = 10 K and E_a = 0 kJ/mol constant. (**C**) Varying T_c while keeping T_m = 500 K and E_a = 15 kJ/mol constant. (**D**) Varying T_c while keeping T_m = 500 K and E_a = 0 kJ/mol constant.

We further explored how the three parameters (E_a, T_m and T_c) in the model affected the diffusion-temperature relation in the range of 275–320 K. Interestingly, the diffusion-temperature relation of interacting molecules could be positively or negatively correlated (Fig. 4A&C). For a given T_c = 10 K, the diffusion of interacting molecules became faster at higher temperatures if T_m was low enough ($\lesssim$1500 K); in contrast, with high T_m ($\gtrsim$2000 K), the diffusion of the same molecule was slower at higher temperatures (Fig. 4A). This observation suggested the possible existence of phase transitions. We observed similar transitions for interacting molecules with constant T_m = 500 K but varying T_c. In contrast, such transitions were absent for non-interacting molecules with either constant T_c = 10 K (but varying T_m, Fig. 4B) or constant T_m = 500 K (but varying T_c, Fig. 4D).

To examine the possible phase transitions, we calculated the molecular diffusion coefficients at temperatures in the range of 275–320 K with different parameters ($0 \le E_a \le 60$ kJ/mol, $0 \le T_m < 3000$ K, $0 \le T_c < 250$ K) and computed the Pearson correlation coefficient (ρ_{TD}) between temperature T and diffusion coefficient D. For non-interacting molecules (E_a = 0 kJ/mol), the correlations were negative (Fig. 5A). However, for interacting molecules (E_a = 15, 30, and 60 kJ/mol), the correlations could be negative at higher T_m and T_c values (red areas in Fig. 5) and positive at lower T_m and T_c values (green areas in Fig. 5). These phase diagrams corroborated the observations based on the individual *D-vs-T* curves in Fig. 4. In addition, as the activation energy E_a increased, the phase diagrams showed higher fractions of positive *T–D*

correlations. The transitions were sharp, as the regions of $-0.1 \leq \rho_{TD} \leq +0.1$ were narrow (Fig. 5), which was also confirmed by examining the T_c-dependence of the correlation coefficient at given T_m values (SI Fig. 7A). The phase transition along the activation energy E_a was also sharp, transitioning from negative correlations to positive ones as the activation energy increased (SI Fig. 7B and 7C).

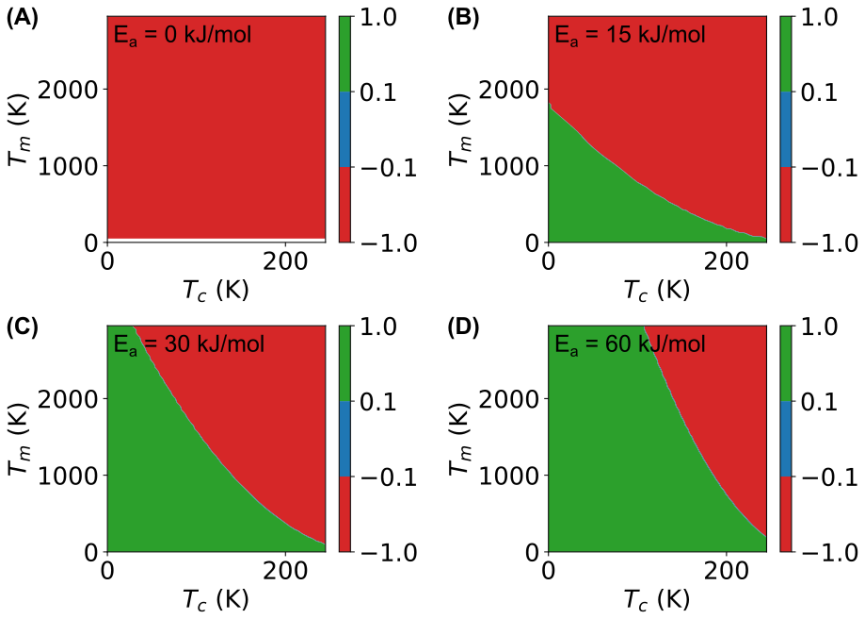

Figure 5. Phase diagrams based on the Pearson correlation coefficient between temperature and molecular diffusion coefficient at different activation energies: (**A**) E_a = 0 kJ/mol, (**B**) E_a = 15 kJ/mol, (**C**) E_a = 30 kJ/mol, and (**D**) E_a = 60 kJ/mol.

To summarize, we applied sptPALM [6] to investigate the diffusion of H-NS proteins and free dyes in bacterial cytoplasm at different temperatures. Although the diffusion of H-NS proteins in both live and dead bacteria increased as temperature increases, appearing to follow the Arrhenius equation instead of the Stokes-Einstein equation, the diffusion of free dyes decreased at higher temperatures, questioning the previously proposed theories based on superthermal fluctuations [17]. To understand the measured diffusion-temperature relations, we developed an alternative model based on free-volume theory, in which the bacterial cytoplasm is considered as a polymeric network. In our model, the Stokes-Einstein equation remains valid, while the polymeric network contributes a significant term to the viscosity. Our model was successful in predicting the diffusion-temperature relations for both H-NS proteins and free dyes inside bacteria. In addition, we systematically examined the predicted diffusion-temperature relations with different parameters in the model, and predicted the possible existence of phase transitions.

Although it was proposed previously that the Stokes-Einstein equation may be invalid in live systems, due to the biological activities, injection of energies due to biochemical reactions, and other active

processes [17–19]. Our work suggested that it is not necessary to violate the Stokes-Einstein equation. This study presents an alternative model by taking into account the polymeric nature of the bacterial cytoplasm and interactions among molecules and polymeric networks. This alternative model provides a theoretical foundation for estimating the material properties (i.e., viscoelasticity) of live systems using the generalized Stokes-Einstein equation [7,30,32,33].

Despite the success of our model for understanding the current data, the model could be further verified. We attributed the difference in the diffusion-temperature relations of H-NS proteins and free dyes mainly to the difference of their interactions with the polymeric network in the bacteria in the current study; however, other factors, such as size and electric charge, may play a role. It would be an ideal experiment to rule out the other contributions by using the same molecule but with different binding affinities to the polymer network. Therefore, it would be exciting to measure and compare the temperature-dependence of diffusion of different H-NS mutants in live bacteria. It would also be interesting to reconstitute the polymeric network *in vitro* and reproduce the diffusion-temperature relation using artificial molecules or nanoparticles whose interactions with the polymeric network can be conveniently modulated. Although the phase transitions predicted by the model were examined using numerical calculations in the current work, it is possible to analytically investigate the phase diagrams. It would also be exciting to experimentally verify the phase transitions predicted by our model. Artificial systems consisting of nanoparticles of different sizes or different strengths of interactions with the polymeric network may contribute to this direction.

Acknowledgment

This work was supported by the National Science Foundation (Grant No. 1826642) and the Arkansas Biosciences Institute (Grants No. ABI-0189, ABI-0226, ABI-0277, ABI-0326, ABI-2021, and ABI-2022). We thank Joshua N. Milstein for the generous gift of the pHNS-mEos3.2 and pHNS plasmids. We are also grateful for support from the Arkansas High Performance Computing Center (AHPCC), which is funded in part by the National Science Foundation (grants no. 0722625, 0959124, 0963249, and 0918970) and the Arkansas Science and Technology Authority.

References

[1] B. R. Parry, I. V. Surovtsev, M. T. Cabeen, C. S. O'Hern, E. R. Dufresne, and C. Jacobs-Wagner, *The Bacterial Cytoplasm Has Glass-like Properties and Is Fluidized by Metabolic Activity.*, Cell **156**, 183 (2014).

[2] S. Cayley, B. A. Lewis, H. J. Guttman, and M. T. Record, *Characterization of the Cytoplasm of Escherichia Coli K-12 as a Function of External Osmolarity. Implications for Protein-DNA Interactions in Vivo.*, J. Mol. Biol. **222**, 281 (1991).

[3] S. B. Zimmerman and S. O. Trach, *Estimation of Macromolecule Concentrations and Excluded Volume Effects for the Cytoplasm of Escherichia Coli.*, J. Mol. Biol. **222**, 599 (1991).

[4] Tortora, G. J. ; Funke, B. R. ; Case, and L. Christine, *Microbiology: An Introduction*, 12th ed. (Pearson, Boston, 2016).
[5] U. Moran, R. Phillips, and R. Milo, *SnapShot: Key Numbers in Biology.*, Cell **141**, 1262 (2010).
[6] S. Manley, J. M. Gillette, G. H. Patterson, H. Shroff, H. F. Hess, E. Betzig, and J. Lippincott-Schwartz, *High-Density Mapping of Single-Molecule Trajectories with Photoactivated Localization Microscopy.*, Nat. Methods **5**, 155 (2008).
[7] A. A. Sadoon and Y. Wang, *Anomalous, Non-Gaussian, Viscoelastic, and Age-Dependent Dynamics of Histonelike Nucleoid-Structuring Proteins in LiveEscherichia Coli*, Phys. Rev. E **98**, 042411 (2018).
[8] A. A. Sadoon, P. Khadka, J. Freeland, R. K. Gundampati, R. H. Manso, M. Ruiz, V. R. Krishnamurthi, S. K. Thallapuranam, J. Chen, and Y. Wang, *Silver Ions Caused Faster Diffusive Dynamics of Histone-Like Nucleoid-Structuring Proteins in Live Bacteria.*, Appl. Environ. Microbiol. **86**, (2020).
[9] Z. W. Zhao, M. D. White, Y. D. Alvarez, J. Zenker, S. Bissiere, and N. Plachta, *Quantifying Transcription Factor-DNA Binding in Single Cells in Vivo with Photoactivatable Fluorescence Correlation Spectroscopy.*, Nat. Protoc. **12**, 1458 (2017).
[10] G. Kaur, M. W. Costa, C. M. Nefzger, J. Silva, J. C. Fierro-González, J. M. Polo, T. D. M. Bell, and N. Plachta, *Probing Transcription Factor Diffusion Dynamics in the Living Mammalian Embryo with Photoactivatable Fluorescence Correlation Spectroscopy.*, Nat. Commun. **4**, 1637 (2013).
[11] M. Stracy, C. Lesterlin, F. Garza de Leon, S. Uphoff, P. Zawadzki, and A. N. Kapanidis, *Live-Cell Superresolution Microscopy Reveals the Organization of RNA Polymerase in the Bacterial Nucleoid.*, Proc. Natl. Acad. Sci. U. S. A. **112**, E4390 (2015).
[12] S. Bakshi, A. Siryaporn, M. Goulian, and J. C. Weisshaar, *Superresolution Imaging of Ribosomes and RNA Polymerase in Live Escherichia Coli Cells.*, Mol. Microbiol. **85**, 21 (2012).
[13] K. J. Barns and J. C. Weisshaar, *Single-Cell, Time-Resolved Study of the Effects of the Antimicrobial Peptide Alamethicin on Bacillus Subtilis.*, Biochim. Biophys. Acta **1858**, 725 (2016).
[14] C. C. Miller and J. Walker, *The Stokes-Einstein Law for Diffusion in Solution*, Proc. R. Soc. Lond. Ser. Contain. Pap. Math. Phys. Character **106**, 724 (1924).
[15] A. Einstein, *Über Die von Der Molekularkinetischen Theorie Der Wärme Geforderte Bewegung von in Ruhenden Flüssigkeiten Suspendierten Teilchen*, Ann. Phys. **322**, 549 (1905).
[16] U. M. B. Marconi, A. Puglisi, L. Rondoni, and A. Vulpiani, *Fluctuation–Dissipation: Response Theory in Statistical Physics*, Phys. Rep. **461**, 111 (2008).
[17] S. C. Weber, A. J. Spakowitz, and J. A. Theriot, *Nonthermal ATP-Dependent Fluctuations Contribute to the in Vivo Motion of Chromosomal Loci.*, Proc. Natl. Acad. Sci. U. S. A. **109**, 7338 (2012).
[18] A. Caspi, R. Granek, and M. Elbaum, *Enhanced Diffusion in Active Intracellular Transport.*, Phys. Rev. Lett. **85**, 5655 (2000).
[19] A. W. C. Lau, B. D. Hoffman, A. Davies, J. C. Crocker, and T. C. Lubensky, *Microrheology, Stress Fluctuations, and Active Behavior of Living Cells*, Phys. Rev. Lett. **91**, 198101 (2003).
[20] P. B. Macedo and T. A. Litovitz, *On the Relative Roles of Free Volume and Activation Energy in the Viscosity of Liquids*, J. Chem. Phys. **42**, 245 (1965).
[21] N. Bag, D. H. X. Yap, and T. Wohland, *Temperature Dependence of Diffusion in Model and Live Cell Membranes Characterized by Imaging Fluorescence Correlation Spectroscopy*, Biochim. Biophys. Acta BBA - Biomembr. **1838**, 802 (2014).
[22] W. L. C. Vaz, R. M. Clegg, and D. Hallmann, *Translational Diffusion of Lipids in Liquid Crystalline Phase Phosphatidylcholine Multibilayers. A Comparison of Experiment with Theory*, Biochemistry **24**, 781 (1985).
[23] P. F. F. Almeida and W. L. C. Vaz, *Chapter 6 - Lateral Diffusion in Membranes*, in *Handbook of Biological Physics*, edited by R. Lipowsky and E. Sackmann, Vol. 1 (North-Holland, 1995), pp. 305–357.
[24] C. J. Dorman, *H-NS: A Universal Regulator for a Dynamic Genome.*, Nat. Rev. Microbiol. **2**, 391 (2004).

[25] J. Sambrook, *Molecular Cloning: A Laboratory Manual, Third Edition (3 Volume Set)*, 3rd ed. (Cold Spring Harbor Laboratory Press, Cold Spring Harbor, N.Y, 2001).
[26] S. C. Weber, A. J. Spakowitz, and J. A. Theriot, *Bacterial Chromosomal Loci Move Subdiffusively through a Viscoelastic Cytoplasm.*, Phys. Rev. Lett. **104**, 238102 (2010).
[27] B. H. A. Rehm, *Bacterial Polymers: Biosynthesis, Modifications and Applications*, Nat. Rev. Microbiol. **8**, 578 (2010).
[28] Y. Xiang, I. V. Surovtsev, Y. Chang, S. K. Govers, B. R. Parry, J. Liu, and C. Jacobs-Wagner, *Solvent Quality and Chromosome Folding in Escherichia Coli*, BioRxiv (2020).
[29] Q. Zhao and S. Matsukawa, *Estimation of the Hydrodynamic Screening Length in κ-Carrageenan Solutions Using NMR Diffusion Measurements*, Polym. J. **44**, 901 (2012).
[30] W. Pan, L. Filobelo, N. D. Q. Pham, O. Galkin, V. V. Uzunova, and P. G. Vekilov, *Viscoelasticity in Homogeneous Protein Solutions.*, Phys. Rev. Lett. **102**, 058101 (2009).
[31] D. C. Grainger, *Structure and Function of Bacterial H-NS Protein.*, Biochem. Soc. Trans. **44**, 1561 (2016).
[32] D. Wirtz, *Particle-Tracking Microrheology of Living Cells: Principles and Applications.*, Annu. Rev. Biophys. **38**, 301 (2009).
[33] T. G. Mason, *Estimating the Viscoelastic Moduli of Complex Fluids Using the Generalized Stokes–Einstein Equation*, Rheol. Acta **39**, 371 (2000).
[34] See Supplemental Material at http://link.aps.org/supplemental/xxx for detailed "Materials and Methods" and supplementary figures, which includes additional Refs. [35–45].
[35] T. Baba, T. Ara, M. Hasegawa, Y. Takai, Y. Okumura, M. Baba, K. A. Datsenko, M. Tomita, B. L. Wanner, and H. Mori, *Construction of Escherichia Coli K-12 in-Frame, Single-Gene Knockout Mutants: The Keio Collection.*, Mol. Syst. Biol. **2**, 2006.0008 (2006).
[36] M. Alqahtany, P. Khadka, I. Niyonshuti, V. R. Krishnamurthi, A. A. Sadoon, S. D. Challapalli, J. Chen, and Y. Wang, *Nanoscale Reorganizations of Histone-like Nucleoid Structuring Proteins in Escherichia Coli Are Caused by Silver Nanoparticles*, Nanotechnology **30**, 385101 (2019).
[37] M. Zhang et al., *Rational Design of True Monomeric and Bright Photoactivatable Fluorescent Proteins.*, Nat. Methods **9**, 727 (2012).
[38] Y. Wang, P. Penkul, and J. N. Milstein, *Quantitative Localization Microscopy Reveals a Novel Organization of a High-Copy Number Plasmid.*, Biophys. J. **111**, 467 (2016).
[39] V. R. Krishnamurthi, J. Chen, and Y. Wang, *Silver Ions Cause Oscillation of Bacterial Length of Escherichia Coli.*, Sci. Rep. **9**, 11745 (2019).
[40] A. Edelstein, N. Amodaj, K. Hoover, R. Vale, and N. Stuurman, *Computer Control of Microscopes Using MManager.*, Curr. Protoc. Mol. Biol. **Chapter 14**, Unit14.20 (2010).
[41] A. D. Edelstein, M. A. Tsuchida, N. Amodaj, H. Pinkard, R. D. Vale, and N. Stuurman, *Advanced Methods of Microscope Control Using MManager Software.*, J. Biol. Methods **1**, (2014).
[42] S. Wolter, A. Löschberger, T. Holm, S. Aufmkolk, M.-C. Dabauvalle, S. van de Linde, and M. Sauer, *RapidSTORM: Accurate, Fast Open-Source Software for Localization Microscopy.*, Nat. Methods **9**, 1040 (2012).
[43] D. B. Allan, T. Caswell, N. C. Keim, and C. M. van der Wel, *Trackpy: Trackpy V0.4.1*, Zenodo (2018).
[44] J. C. Crocker and D. G. Grier, *Methods of Digital Video Microscopy for Colloidal Studies*, J. Colloid Interface Sci. **179**, 298 (1996).
[45] C. A. Schneider, W. S. Rasband, and K. W. Eliceiri, *NIH Image to ImageJ: 25 Years of Image Analysis.*, Nat. Methods **9**, 671 (2012).

Supplementary Information

Revisiting the temperature dependence of protein diffusion inside bacteria: validity of the Stokes-Einstein equation

Asmaa A. Sadoon[a,b,d], William F. Oliver[a,b], and Yong Wang[a,b,c,*]

[a] Department of Physics, [b] Materials Science & Engineering Program, [c] Cell and Molecular Biology Program, University of Arkansas, Fayetteville, Arkansas, 72701, USA. [d] Department of Physics, University of Thi-Qar, Thi-Qar, Iraq.

*Corresponding author: yongwang@uark.edu

Materials and Methods

Bacterial strains

E. coli strain JW1225 from the Keio collection [35] was used in this study. This strain lacked the *hns* gene and thus was transformed with either pHNS-mEos3.2 plasmid or pHNS plasmid. Both plasmids encode the *hns* gene, but the *hns* gene was fused to the *meos3.2* gene in the pHNS-mEos3.2 plasmid. The strain (JW1225 + pHNS-mEos3.2) was used in our previous studies [7,8,36], expressing H-NS proteins fused to mEos3.2 photo-switchable fluorescent proteins [37], which allowed us to perform single-particle tracking photoactivated localization microscopy (sptPALM) on the H-NS proteins [6–8,36]. The other strain (JW1225 + pHNS) was non-fluorescent and thus suitable for tracking free dyes.

Bacterial growth and sample preparation for tracking H-NS proteins in live bacteria

The bacteria (JW1225 + pHNS-mEos3.2) were grown overnight in a defined M9 minimal medium, supplemented with 1% glucose, 0.1% casamino acids, 0.01% thiamine and appropriate antibiotics (kanamycin and chloramphenicol) at 37ºC in a shaking incubator with a speed of 250 rpm [7,8,36,38,39]. On the next day, the overnight culture was diluted by 50 to 100 times into fresh medium such that OD_{600} = 0.05. This culture (5 mL) was regrown in the shaking incubator at 37ºC for 2–3 hr. When the OD_{600} of the new bacterial culture reached 0.3, 10 μL of the bacteria were transferred onto a small square of agarose pad (5 mm × 5 mm), followed by incubation in dark at room temperature (21ºC) for 30 min to allow bacteria to be absorbed onto the agarose pad. The pad was then flipped and placed to a clean glass coverslip at the bottom of a petri-dish, which was mounted inside a stage-top incubator (Okolab, Ambridge, PA) on our microscope for imaging.

Bacterial growth and sample preparation for tracking free dyes in dead bacteria

The bacteria (JW1225 + pHNS) were grown as described above, and converted to electrocompetent cells following standard protocols [25]. Then, 30 μL of the competent cells were mixed gently with 2 μL of PA Janelia Fluor 646 dyes (0.2 mM in dimethyl sulfoxide), incubated on ice for 2 min, and transferred into a cold electroporation cuvette with a gap of 1 mm. A pulse of 1.9 kV and 5 ms was applied to deliver the dyes into the bacterial cells [25], followed by add 500 μL of the fresh M9 minimal medium, supplemented with 1% glucose, 0.1% casamino acids, 0.01% thiamine and appropriate antibiotics. After incubation at 37ºC for 1 hour on a shaking incubator (250 rpm), 10 μL of the bacteria were transferred onto a small agarose pad containing SYTOX™ Blue dyes at 3μM (Thermo Fisher Scientific), followed by mounting for imaging as described above.

Bacterial growth and sample preparation for tracking H-NS proteins in dead bacteria

For tracking H-NS proteins in dead bacteria, the bacteria (JW1225 + pHNS-mEos3.2) were prepared and treated by electroporation the same as the sample for tracking free dyes in dead bacteria, except that the PA Janelia Fluor 646 dyes were omitted during the electroporation step.

Single-particle tracking photoactivated localization microscopy (sptPALM)

We performed sptPALM experiments for the H-NS proteins and the free dyes on a super-resolution fluorescence microscope, which was based on an Olympus IX-73 inverted microscope and equipped with an Olympus TIRF 100× N.A. = 1.49 oil immersion objective, a multilaser system (iChrome MLE, TOPTICA Photonics, New York), and an EMCCD camera (Andor, Massachusetts). The fusion proteins of H-NS and mEos3.2 were activated and excited at 405 nm and 532 nm, respectively. For the PA Janelia Fluor 646 dyes, the 405 nm laser and the 640 nm laser from the multilaser system were used as the activation and excitation lasers, respectively. Micro-Manager [40,41] was used for microscope control and data acquisition, with an exposure time of 30 ms. The effective pixel size of acquired images was 160 nm, and the actual interval between frames was 45 ms. The resulting movies (20 000 frames) were analyzed with RapidStorm [42], generating *x/y* positions, *x/y* widths, intensity, and background for each detected fluorescent spot. Spots with localization precisions > 40 nm were rejected [7,8,38]. The positions of the molecules were linked into trajectories using the *trackpy* package [43] with a memory of one frame and a maximum step size of 480 nm [6–8,11,44], followed by calculating the means-square-displacements (MSD) using *trackpy* [43]. At least 44,000 trajectories of single particles were used for analysis at each temperature.

Imaging of dead bacteria stained by SYTOX^{TM} Blue dyes

Bacteria after electroporation were imaged by both brightfield microscopy (exposure time = 30 ms) and fluorescence microscopy (excitation = 405 nm, exposure time = 30 ms) using the Olympus 100× TIRF objective. Multiple fields of views were obtained for each sample. Brightfield and fluorescence images were colored and merged using ImageJ [45]. The numbers of fluorescent bacteria (i.e., dead cells) and non-fluorescent ones (i.e., live cells) were counted manually to estimate the percentage of dead bacteria.

Supplementary Figures

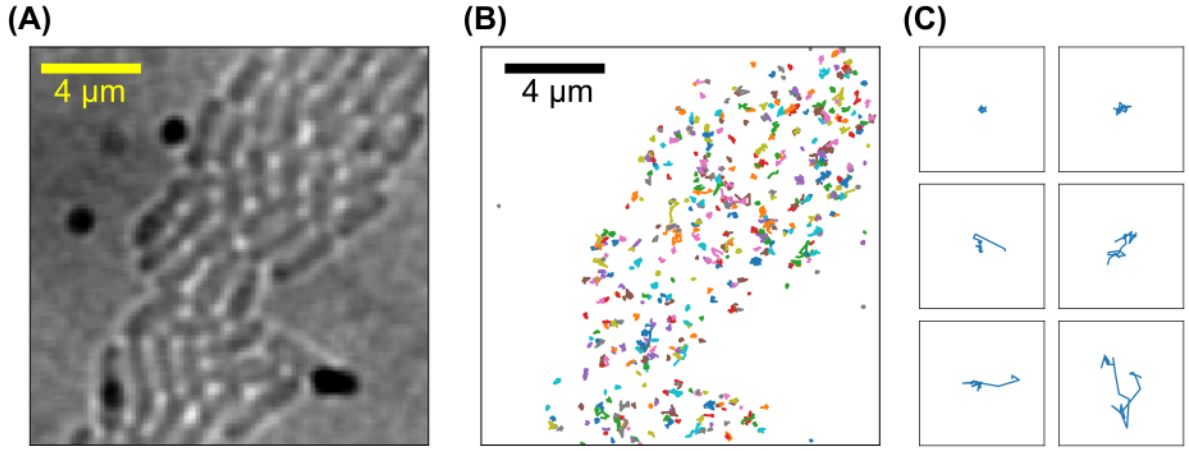

SI Figure 1. Examples of trajectories of H-NS proteins in *E. coli* bacteria. (**A**) A brightfield image of bacteria. (**B**) Trajectories of H-NS proteins in the bacteria shown in panel A. (**C**) Examples of individual trajectories of H-NS proteins. The size of the boxes is 1.6×1.6 μm.

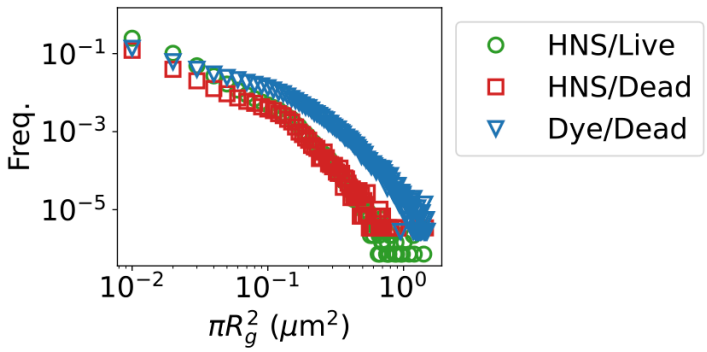

SI Figure 2. Distribution of the explored area (πR_g^2) of individual proteins and dyes based on the radius of gyration (R_g) of individual trajectories.

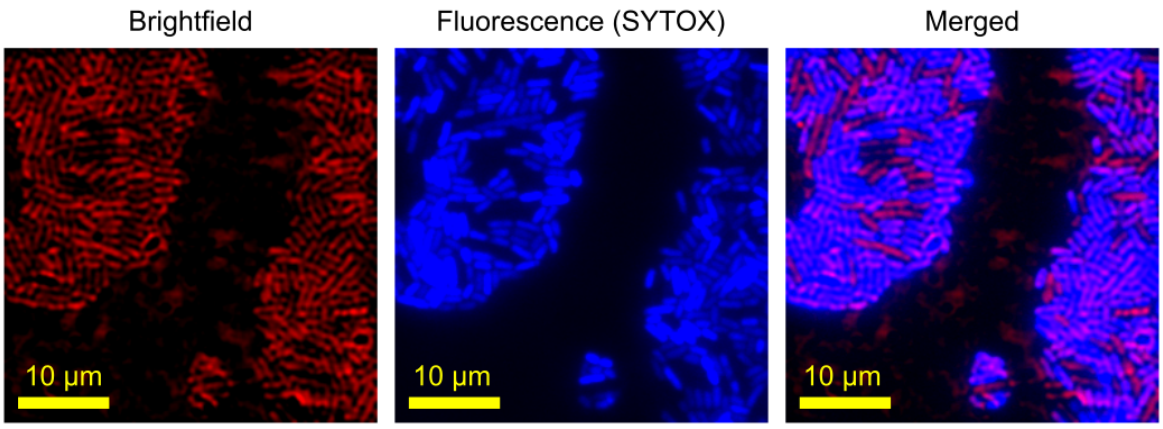

SI Figure 3. Confirmation of the death of bacteria after electric shock and stained by SYTOX™ Blue dyes (blue) overlapped on the corresponding brightfield image (red).

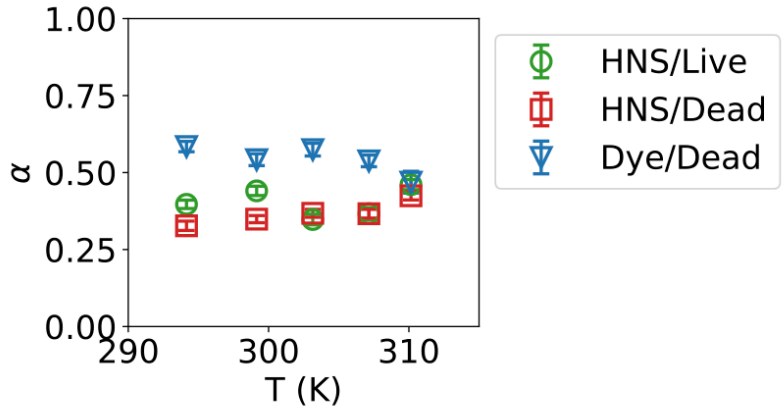

SI Figure 4. Temperature dependence of the sub-diffusive scaling exponent α for the diffusion of H-NS proteins and dyes in bacteria.

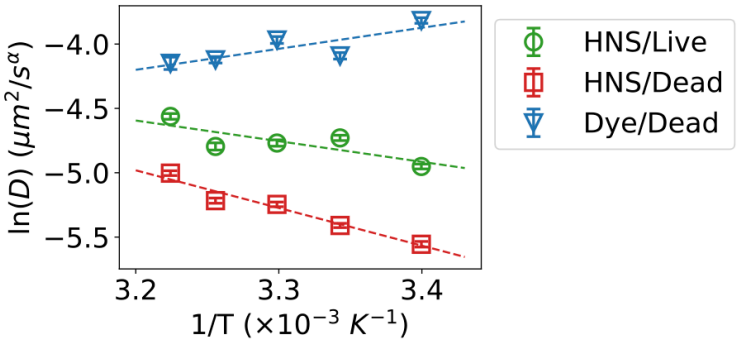

SI Figure 5. Dependence of ln(D) on 1/T for H-NS proteins and dyes in live or dead *E. coli* bacteria. Dashed lines are linear fittings.

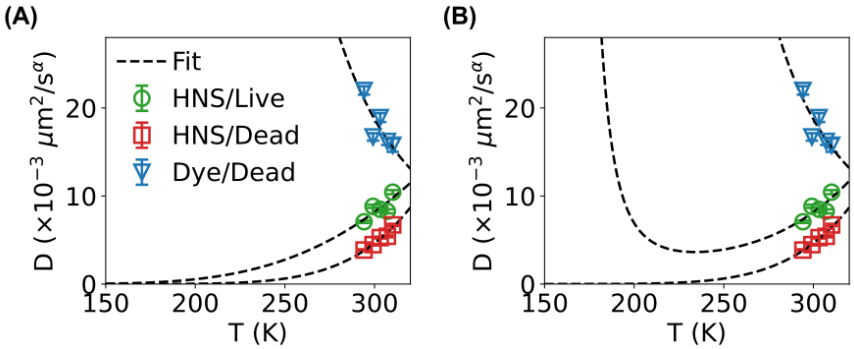

SI Figure 6. Two sets of fitted curves for the same set of experimental data with different T_c bounds of (A) 0 – 10 K and (B) 0 – 100 K. Both sets of the fittings overlapped with the experimental data similarly well. However, the fitted curves were significantly different at lower temperatures.

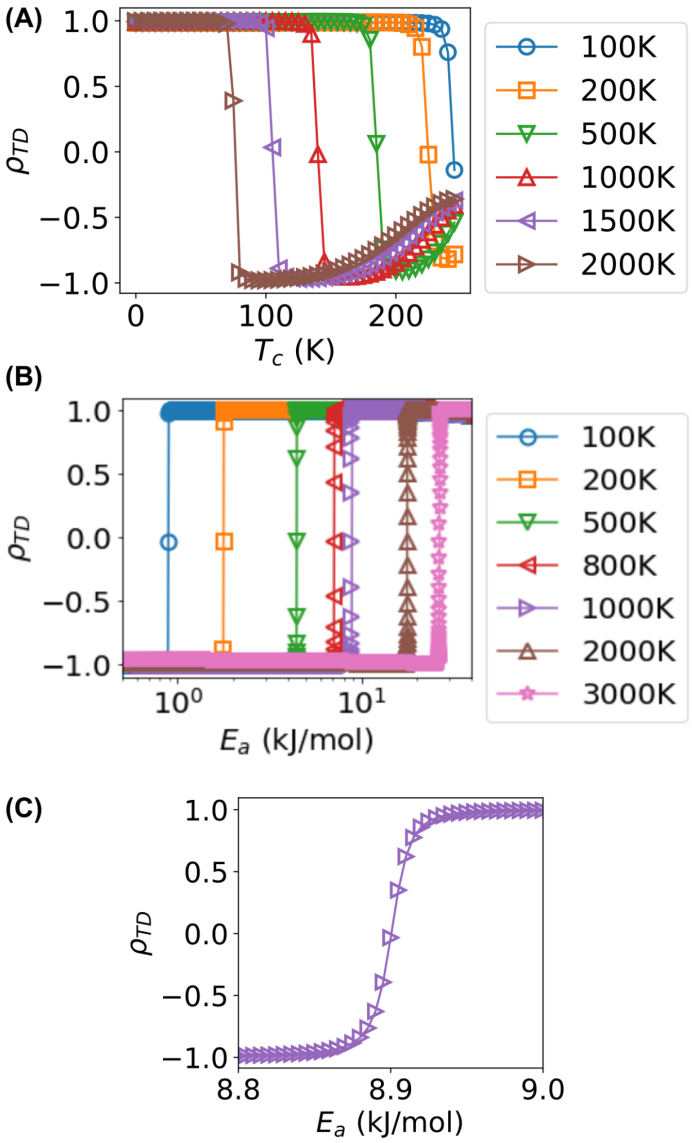

SI Figure 7. Sharp transitions predicted from the model. (**A**) Dependence of the diffusion-temperature correlation ρ_{TD} on T_c at different T_m values (shown in legends) but with constant E_a = 30 kJ/mol. (**B**) Dependence of the diffusion-temperature correlation ρ_{TD} on E_a at different T_m values (shown in legends) but with constant T_c = 10 K. (**C**) A closer look at the same data in panel B with T_c = 10 K and T_m = 1000 K.